



The knockout of tobacco *NtCBL10* inhibits leaf Cl^- accumulation and leads to light-dependent necrosis & light-independent chlorosis under salt stress

Jingjing Mao^{a,b,c,d,e}, Guang Yuan^{a,b}, Richard G.F. Visser^c, Yuling Bai^c, Gang Xu^f, Lin Xue^f, Dongping Mao^f, Haobao Liu^a, Yang Ning^{a,*}, Qian Wang^{a,*}, C. Gerard van der Linden^c

^a Tobacco Research Institute, Chinese Academy of Agricultural Sciences (CAAS), Qingdao 266101, PR China

^b Graduate School of Chinese Academy of Agricultural Sciences (GSCAAS), Beijing 100081, PR China

^c Plant Breeding, Wageningen University & Research (WUR), Wageningen 6708 PB, the Netherlands

^d Graduate School Experimental Plant Sciences, Wageningen University, Wageningen 6708 PB, the Netherlands

^e Technology Centre, China Tobacco Jiangsu Industrial Co., Ltd., Nanjing 210000, PR China

^f Anhui Wannan Tobacco Co., Ltd., Xuancheng 242000, PR China

ARTICLE INFO

Keywords:

CBL10
Salt tolerance
Necrosis
Chlorosis
Light
 Cl^-

ABSTRACT

CBL10 was shown to be a key gene for salt tolerance in *Arabidopsis thaliana*. In this study, we evaluated the role of *CBL10* in the tobacco salt tolerance response by characterizing the gene editing-induced loss-of-function knockout mutants of the two *NtCBL10* homeologous genes *NtCBL10A* and *NtCBL10B*. The importance of *NtCBL10* for the response to salinity was evidenced by the salt supersensitivity of the *Nt-cbl10a10b* double mutants, with fast-developing chlorosis and severe necrotic lesions on leaves. Stomatal conductance and photochemical efficiency of photosystem 2 (PhiPS2) of the *Nt-cbl10a10b* double mutant were significantly inhibited already at a very early stage of the salt stress response. Leaf Na^+ concentrations were not much affected in these plants, but the Cl^- content of the *Nt-cbl10a10b* double mutants was significantly lower than that of wild-type plants, which is the first report of *CBL10* in the regulation of Cl^- homeostasis. Interestingly, the necrosis phenotype of *Nt-cbl10a10b* double mutants was dependent on light, while the chlorosis phenotype of *Nt-cbl10a10b* double mutants was light-independent. Different from the previous studies that focus on the role of *CBL10* in Na^+ homeostasis regulation, this study indicates that *NtCBL10* is a key component in regulating multiple aspects of ion homeostasis under salt stress.

1. Introduction

The Calcineurin B-like Protein—CBL-interacting Protein Kinase (CBL-CIPK) network relays physiological signals characterized by $[\text{Ca}^{2+}]_{\text{cyt}}$ transients, playing essential roles in both plant development and stress adaptation (Mao et al., 2022). In *Arabidopsis thaliana*, several CBL and CIPK family members were reported to be involved in the salt stress response. The most well-known CBL-CIPK pathway is the SOS (salt overly sensitive) pathway: AtCBL4 (AtSOS3) works with AtCIPK24 (AtSOS2) to phosphorylate and activate the plasma membrane (PM)-localized Na^+/H^+ antiporter AtSOS1, leading to Na^+ extrusion from the root cells (Nunez-Ramirez et al., 2012; Qiu et al., 2002; Shi et al., 2002). This pathway is conserved in many other plant species

(Mao et al., 2022).

AtCBL10 has been suggested as an addition to the SOS pathway in plant shoots, but the *in vivo* functional relationship of CBL10 and Na^+ homeostasis remains unclear. Some authors reported that AtCBL10-AtCIPK8/24 complexes positively regulate the activity of PM-localized AtSOS1 to extrude excess Na^+ from plant shoots (Quan et al., 2007, Lin et al., 2009, Yin et al., 2019). Thus, the knockout of *AtCBL10* is supposed to increase Na^+ accumulation in plants, but this conflicts with the observation that *cbl10* mutants accumulate significantly less Na^+ than WT even though they exhibit a salt-sensitive phenotype. Other authors proposed that AtCBL10-AtCIPK24 may promote the Na^+ compartmentalization in the vacuole to explain the salt sensitivity and lower Na^+ accumulation of *At-cbl10* mutants, but the tonoplast-localized

* Corresponding authors.

E-mail addresses: maojingjing40@163.com (J. Mao), yuanguang1995@163.com (G. Yuan), richard.visser@wur.nl (R.G.F. Visser), bai.yuling@wur.nl (Y. Bai), xu2200@163.com (G. Xu), 172804823@qq.com (L. Xue), 605609602@qq.com (D. Mao), liuhaobao@caas.cn (H. Liu), ningyang@caas.cn (Y. Ning), wangqian01@caas.cn (Q. Wang), gerard.vanderlinden@wur.nl (C. Gerard van der Linden).

<https://doi.org/10.1016/j.envexpbot.2024.106083>

Received 25 May 2024; Received in revised form 8 November 2024; Accepted 30 December 2024

Available online 6 January 2025

0098-8472/© 2025 The Authors. Published by Elsevier B.V. This is an open access article under the CC BY-NC license (<http://creativecommons.org/licenses/by-nc/4.0/>).

targets remain uncertain (Kim et al., 2007, Plasencia et al., 2020). Potential candidates for the targets include the Na^+/H^+ exchanger (NHX) and H^+ pumps (AVP1, VHA) (Kim et al., 2007, Plasencia et al., 2020). In addition to its localization at PM and tonoplast, AtCBL10 has also been reported to interact with the TOC34 (Translocon of the Outer Membrane of the Chloroplasts 34), a GTP-dependent receptor at the outer membrane of chloroplasts (Cho et al., 2016). These studies hint that AtCBL10 might play multiple roles in adapting ion homeostasis under saline conditions, contingent upon its subcellular locations. Therefore, the phenotypic and physiological differences of At-cbl10 mutants under salt stress could be a combined outcome arising from the disruption of multiple CBL10-dependent pathways.

Tobacco (*Nicotiana tabacum*) is relatively salt tolerant, and this tolerance is attributed to a variety of underlying mechanisms (Sun et al., 2020). However, whether tobacco NtCBL10 plays a role in the salt tolerance of tobacco remains to be identified. Recently, we showed that there are 24 NtCBL genes in *N. tabacum* (Mao et al., 2023). Among these genes are two AtCBL10 orthologs: NtCBL10A and NtCBL10B, with their origins traced back to the maternal diploid tobacco species *N. sylvestris* and paternal diploid tobacco species *N. tomentosiformis*, respectively (Mao et al., 2023). NtCBL10A and NtCBL10B are predominantly expressed in the shoots, with expression levels gradually decreasing across the leaf blade, main vein, stem, and root tissues (Mao et al., 2023). NtCBL10A exhibits a significantly higher overall expression level, approximately threefold higher than NtCBL10B (Mao et al., 2023). In addition, the gene expression levels of both NtCBL10A and NtCBL10B were upregulated in the leaf blade but not in the root under 100 mM NaCl stress (Mao et al., 2023).

To gain further insight into the role of CBL10 in the salt tolerance of tobacco, we constructed gene editing-induced loss-of-function mutants of NtCBL10A and NtCBL10B (premature stop codons) and evaluated their salt tolerance in this study. Our results demonstrate that NtCBL10 is indeed a key component in the salt tolerance of tobacco, and indicate that the lack of NtCBL10 disrupts multiple pathways associated with either severe necrosis or chlorosis symptoms.

2. Materials and methods

2.1. Plant materials and growth conditions

N. tabacum L. cv. Zhongyan 100 cultivar was used as plant material in this study. For determining the expression profiles of NtCBL genes in different tobacco tissues at a young stage, tobacco plants were grown from Dec 2022 to Jan 2023 at Unifarm, Wageningen University & Research in the Netherlands. The conditions of the greenhouse were 16 h light / 8 h dark at 25/23 °C and 70 % relative humidity. The shortwave radiation level was maintained in the greenhouse compartment using artificial PAR (photosynthetically active radiation) when the incoming shortwave radiation was below 200 Wm^{-2} (Mao et al., 2021).

2.2. Plasmids construction

The coding sequence of NtCBL10A was amplified from leaf cDNA synthesized from RNA extracted from leaves of tobacco cultivar Zhongyan 100 with primers NtCBL10A-1F and NtCBL10A-1R (Supplementary Table S1). The amplified sequence was then cloned into the 35S promoter-driven pCHF3 vector, resulting in the binary recombinant vector pCHF3-NtCBL10A.

To construct the gene knockout plasmid, CRISPR single guide RNAs (sgRNAs) (Supplementary Table S1) were designed using the online tool CRISPR MultiTargeter (<http://www.multicrispr.net/index.html>) (Zhou and Xu, 2023). Unique sgRNA targets within the coding sequences of NtCBL10A and NtCBL10B were selected to generate Nt-cbl10a and Nt-cbl10b single mutants, respectively. For the construction of the Nt-cbl10a10b double mutant, a common sgRNA target in both NtCBL10A and NtCBL10B coding sequences was chosen. The sgRNA fragments

were synthesized and inserted at the BsaI site of the pDC45 vector (Li et al., 2022) using T4 ligase (Accurate Biotechnology (Human) Co., Ltd, Cat No./ID: AG11801, Changsha, China), resulting in the plasmids pDC45-NtCBL10A, pDC45-NtCBL10B, and pDC45-NtCBL10. All constructs were verified through DNA sequencing by the BGI company, and the confirmed plasmids were transformed into *Agrobacterium tumefaciens* EHA105 for tobacco transformation.

2.3. Generation of NtCBL10A-overexpressing (NtCBL10AOE) plant

To generate the gene overexpressing lines, *Agrobacterium* carrying the pCHF3-NtCBL10A plasmid was introduced into cultivar Zhongyan 100 by the *Agrobacterium*-mediated leaf disc transformation method (Horsch et al., 1985). To screen for NtCBL10AOE lines, positive transgenic plants of the T0 generation were identified by PCR with the primers NtCBL10-1F and pCHF3-R (Supplementary Table S1). The endogenous and exogenous NtCBL10A expression levels of two NtCBL10AOE lines were measured with Real-time quantitative PCR (RT-qPCR) using primer pairs NtCBL10A-qF/NtCBL10-qR and NtCBL10A-qF-2/pCHF3-Allcheck-2 (Supplementary Table S1), respectively. The reference gene is NtL25 (Schmidt and Delaney, 2010).

For homozygous lines selection, more than 200 T1 seeds from T0 NtCBL10AOE plants with high gene overexpression levels were harvested and subsequently screened on the selection medium (1/2 MS medium with 50 $\mu\text{g}/\text{ml}$ kanamycin). Two T1 lines (OE-1 and OE-16) with a segregation of around 3:1 (tolerance: sensitivity) were selected for harvesting T2 seeds. More than 200 T2 seeds were screened on the selection medium again. The T2 generation with 100 % kanamycin resistance was considered as homozygous plants with 100 % kanamycin resistance in the T2 generation were used for the evaluation of stress tolerance.

2.4. Generation of gene knockout mutants

To generate the gene knockout lines, *Agrobacterium* carrying the pDC45-NtCBL10A, pDC45-NtCBL10B, and pDC45-NtCBL10 plasmids were introduced into Zhongyan 100 by the *Agrobacterium*-mediated leaf disc transformation method (Horsch et al., 1985). The selection of plants carrying mutations in NtCBL10 was done by analyses of PCR products flanking the sgRNA target regions. PCR using primers pDC45-NtCBL10A-JCF/pDC45-NtCBL10A-JCR (for NtCBL10A) and pDC45-NtCBL10B-JCF/pDC45-NtCBL10B-JCR (for NtCBL10B) (Supplementary Table S1) yielded a 462 bp and a 607 bp product flanking the sgRNAs, respectively. The PCR products were deep sequenced to further characterize the mutation events, the data were collected and analyzed using the Hi-TOM platform (Liu et al., 2019). *Nicotiana tabacum* is an allotetraploid (e.g., AABB genotype). For the single mutants (Nt-cbl10a, Nt-cbl10b), homozygous plants (aaBB, AAbb) can be obtained from the primary transformants (T1 progeny). To generate the double mutant Nt-cbl10a10b (aabb), aaBb or Aabb plants from the T1 progeny were selected and then self-pollinated to produce the T2 progeny. The single mutants (T1 progeny) with aaBB and AAbb genotypes, as well as the double mutants (T2 progeny) with the aabb genotype, were used for the salt treatment experiments.

2.5. Application and phenotyping of salt treatment

Tobacco seeds were first sown in the soil. At 20 days after germination (DAG), the young tobacco plants were transplanted in rock-wool plugs within float trays for hydroponic cultivation (1/2 Hoagland's nutrient solution). After 6 days of acclimatization (at ~26 DAG), plants were transplanted to a circular flow hydroponic system filled with 1/2 Hoagland's nutrient solution (500 L). The 1/2 Hoagland's nutrient solution under control conditions contained trace amounts of Na^+ and Cl^- (5.51 $\mu\text{g}/\text{ml}$ and 7.88 $\mu\text{g}/\text{ml}$, respectively), measured using the Ion Chromatography (IC) system 850 Professional (Metrohm, Switzerland).

After 6 days of acclimatization (at ~ 32 DAG), NaCl was added to the nutrient solution to a concentration of 50 mM on the first day to reduce salt shock, and 100 mM NaCl concentration was reached the next day. Starting from the day of the 100 mM NaCl treatment, photographs of the selected leaves from different lines were taken daily until harvest.

2.6. Parameters measurement

To assess salt tolerance, chlorophyll content was measured with the Apogee MC-100 Chlorophyll Meter (Masaló and Oca, 2020). Stomatal conductance (gsw), quantum efficiency of PSII (PhiPS2), and leaf transpiration (E_{apparent}) were measured with the LI-600 Porometer/Fluorometer (Price, 2021), which is designed to assess two key aspects of leaf photosynthesis. The porometer calculates stomatal conductance by measuring the mass balance of water vapor flux from the leaf, while the fluorometer uses optical techniques to measure the quantum efficiency of PSII (PhiPS2) in a light-adapted state ($(F'_m - F_s)/F'_m$). Necrosis quantification was performed using ImageJ software (<https://imagej.net/ij/index.html>), as detailed in Góral, (2023). By measuring the total leaf area and the necrotic area, the percentage of necrosis was calculated.

2.7. Ion content measurement

For ion content measurement, the leaves (without main veins) of the whole plant were collected and dried at 105 °C until a stable weight was achieved, and the dry tissue was then ground into powder. Approximately 30–50 mg of the dry sample was placed into a test tube. The powdered samples were ashed at 650 °C for 6 h. One milliliter of 3 M formic acid was added to the test tube, which was then shaken for 20 min at 5000 rpm at 99.9 °C. Subsequently, 9 ml of Milli-Q® water was added to the test tube and mixed. A 0.2 ml sample was taken and diluted with 9.8 ml of Milli-Q® water, resulting in a 50-fold dilution. The ion contents of the diluted samples were measured using the Ion Chromatography (IC) system 850 Professional (Metrohm, Switzerland). The ion contents are expressed based on a dry weight (DW) basis.

2.8. Application of dark treatment

For the dark treatment, whole plants were covered with light-tight black trays at the same time as the initiation of the salt treatment.

2.9. Real-time quantitative PCR

For RT-qPCR, total RNA was extracted from leaves using the RNeasy Plus Mini Kit (Qiagen, Cat No./ID:74134) and purified according to the manufacturer's protocol. RNA was reverse transcribed into cDNA using Evo M-MLV Mix Kit with gDNA Clean for qPCR (Accurate Biotechnology (Hunan) Co., Ltd, Cat No./ID: AG11728, Changsha, China), and the cDNA was amplified using SYBR Green Pro Taq HS qPCR Premix (Accurate Biotechnology (Hunan) Co., Ltd, Cat No./ID: AG11701, Changsha, China) on the LightCycler® 96 Instrument (F. Hoffmann-La Roche Ltd, Switzerland). Amplification reactions were carried out in a total volume of 10 µl, containing 5 µl 2 × SYBR Green Pro Taq HS qPCR Premix, 0.6 µl forward and reverse primers (10 µM), 1 µl cDNA (10 times diluted), and 3.4 µl ddH₂O. The RT-qPCR amplification program was as follows: 95 °C for 10 min, followed by 40 cycles of amplification at 95 °C for 10 s, 60 °C for 30 s. Relative gene expression data were analyzed using the 2- $\Delta\Delta C_t$ method (Livak and Schmittgen, 2001).

2.10. Statistical analysis

Statistical analysis was done using IBM SPSS Statistics 23 software. Significant differences were examined by Student's *t*-test or one-way ANOVA with LSD test at $p < 0.05$ and $p < 0.01$. The figures were drawn by GraphPad Prism 6.0.

3. Results

1. Two *NtCBL10* homeologous genes in tetraploid tobacco

The role of *CBL10* in the salt stress response has been explored through gene knockout mutants of *Arabidopsis thaliana* (Kim et al., 2007, Quan et al., 2007) and *Solanum lycopersicum* (Egea et al., 2018), as well as gene knockdown mutants of *Eutrema salsugineum* (Monihan et al., 2019). The amino acid sequences of the CBL10 proteins in these species were compared to those of NtCBL10A and NtCBL10B from tobacco (Fig. 1). Results showed that all of these CBL10 proteins exhibit highly conserved Ca²⁺-binding domains, suggesting that their ability for Ca²⁺-binding is conserved. However, their N-terminal sequences display significant variability, even though all these CBL10 proteins are predicted to possess a transmembrane domain and the key Cys (C) residue for membrane localization (Fig. 1). A study of *EsCBL10a* and *EsCBL10b* revealed that the differences in the N-terminal domain differentiate their abilities to activate and complement the SOS pathway (Monihan et al., 2019). The variable N-terminal sequences of CBL10 proteins in different plant species may reflect differences in their roles in the salt stress response.

2. Loss-of-function mutants of *NtCBL10* exhibit a salt supersensitive phenotype

To further explore the role of *NtCBL10* in the salt tolerance of tobacco, we generated both gene overexpression and gene knockout lines. For the gene overexpression lines, we focused on constructing *NtCBL10AOE* lines (Supplementary Fig.S3) because *NtCBL10A* exhibits a significantly higher overall expression level (Mao et al., 2023) and the two NtCBL10 proteins differ by only three amino acids (Supplementary Fig.S1). Two independent homozygous *NtCBL10AOE* lines were obtained and both were included in this study. For the gene knockout lines, we obtained two independent homozygous *Nt-cbl10a* lines (Supplementary Fig.S2A), one homozygous *Nt-cbl10b* line (Supplementary Fig.S2B), and one homozygous double mutant line *Nt-cbl10a10b* (Supplementary Fig.S2C) using the CRISPR/Cas9 technique. All the gene editing-induced mutations resulted in the premature termination of protein translation (Supplementary Fig.S2).

The salt tolerance of the knockout mutants as well as *NtCBL10AOE* lines were evaluated in a hydroponic system, with a 100 mM NaCl salt stress treatment. At 7 DAT (days after reaching 100 mM NaCl treatment), the phenotype and growth characteristics of all the transgenic and mutant lines grown under control conditions were similar to WT plants (Fig. 2). Under salt stress, however, the *Nt-cbl10a* and *Nt-cbl10b* single mutants exhibited chlorotic spots on their leaves, and the *Nt-cbl10a10b* double mutant even showed extremely fast-developing severe chlorosis with necrotic lesions (Fig. 2A; Supplementary Fig.S4). In addition, the growth vigor of the *Nt-cbl10a10b* double mutant was significantly reduced under salt stress compared to WT plants (Fig. 2B–2E). These results clearly indicate that *NtCBL10A* and *NtCBL10B* play a key role in the salt tolerance of tobacco and they may be (at least partly) functionally redundant. The *Nt-cbl10a* single mutants exhibited earlier and more severe salt-sensitive phenotype than the *Nt-cbl10b* single mutant (Supplementary Fig.S4), which is consistent with the higher expression level of *NtCBL10A* compared to *NtCBL10B* (Mao et al., 2023). The phenotypes and growth characteristics of the *NtCBL10AOE* lines were not significantly different from the WT plants (Fig. 2).

3. Physiological response to salt stress of *NtCBL10* loss-of-function mutants

For the physiological characterization of the salt response of the *NtCBL10* loss-of-function mutants, we measured the chlorophyll content, stomatal conductance, and photochemical efficiency of photosystem 2 (PhiPS2) at 3 DAT and 7 DAT. The chlorophyll content of the

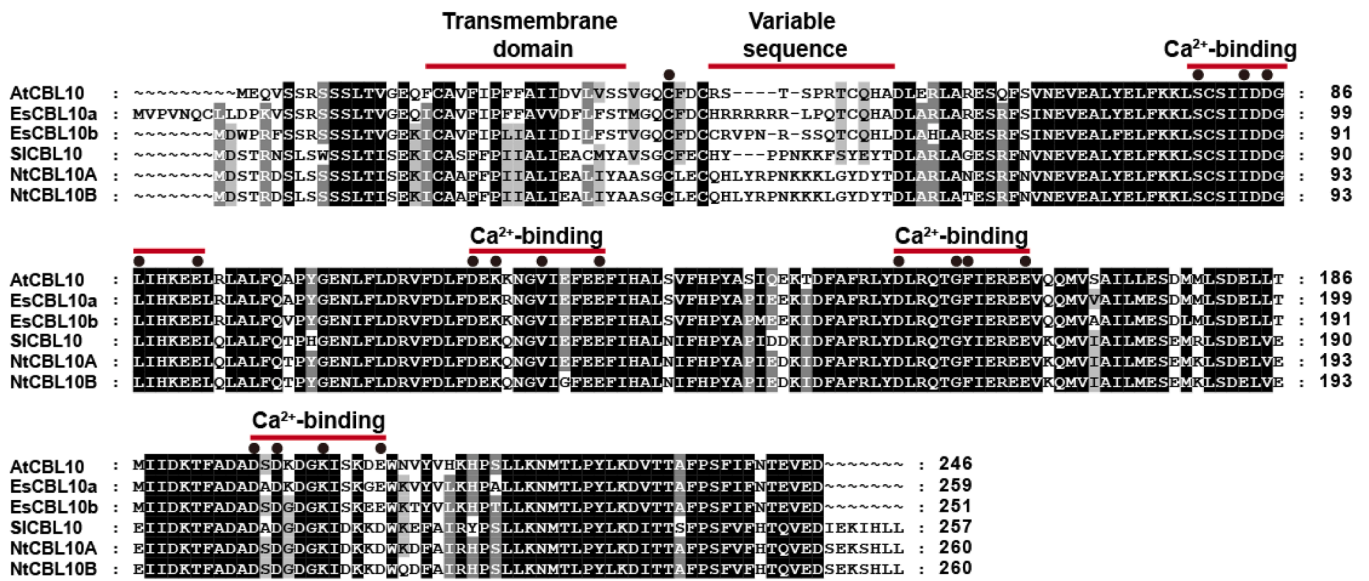


Fig. 1. Phylogenetic tree and protein sequence alignments of the CBL10 proteins. (A) Protein sequence alignments of the CBL10 proteins of *Nicotiana tabacum*, *Eutrema salsgineum*, *Populus trichocarpa*, and *Solanum lycopersicum*. The amino acid sequence of AtCBL10 was downloaded from TAIR. The amino acid sequences of EsCBL10a (XP_006412404.1), EsCBL10b (XP_006397081.1), SICBL10 (NP_001239045.1), NtCBL10A (XP_016498333.1), NtCBL10B (XP_016514866.1) were downloaded from NCBI. Transmembrane prediction is conducted by DAS (<https://tmdas.bioinfo.se/>). The position of key Cys (C) residue in CBL10 proteins and the predicted Ca²⁺-binding sites in EF-hand loops were marked with full dots.

Nt-cbl10a10b double mutant was already greatly reduced under salt stress at 3 DAT (Fig. 3A). At 7 DAT, the chlorophyll content of *Nt-cbl10a* and *Nt-cbl10b* single mutants were slightly but significantly reduced by salt stress compared to the WT plants but much less than that of the *Nt-cbl10a10b* double mutant (Fig. 3D). Similarly, stomatal conductance and PhiPS2 of the *Nt-cbl10a10b* double mutant were significantly lower than WT already at 3 DAT (Figs. 3B, 3C). The PhiPS2 of *Nt-cbl10a* and *Nt-cbl10b* single mutants was not significantly reduced at both 3 DAT and 7 DAT compared to WT (Figs. 3C, 3F), indicating that the loss of either *NtCBL10A* or *NtCBL10B* did not severely affect the photosynthetic efficiency of tobacco.

The leaf ion contents of all lines were measured to assess whether changed ion homeostasis would underlie the extreme salt sensitivity of the *NtCBL10* loss-of-function mutants. Leaf Na⁺, Ca²⁺, and Mg²⁺ contents were not significantly different between WT, mutants, and *NtCBL10A*OE lines under both control and saline conditions (Fig. 3G; Supplementary Fig.S5A, S5B). Interestingly, the Cl⁻ content of the *Nt-cbl10a10b* double mutant was significantly lower than that of WT and other mutants under salt stress (Fig. 3H), while the K⁺ content was higher in the double mutant (Fig. 3I).

Our results showed that in the *Nt-cbl10a10b* double mutant, photosynthetic activity was inhibited and chlorophyll breakdown was initiated very shortly after imposing salt stress. We examined this fast-developing phenotypic response of the double mutant in more detail, monitoring changes in photosynthetic parameters and ion contents in the *Nt-cbl10a10b* double mutant and WT tobacco plants every day after imposing 100 mM NaCl stress (0–5 DAT). The chlorophyll content, stomatal conductance, and photochemical efficiency of photosystem 2 (PhiPS2) of *Nt-cbl10a10b* double mutant were affected already at 1 DAT (48 hrs after the first 50 mM NaCl addition at 0 DAT, 24 hrs after reaching 100 mM NaCl) (Fig. 4B–4D). Chlorotic symptoms were visible already at 1 DAT and necrotic spots were visible at 2 DAT (Fig. 4A), further developing chlorosis and necrosis over the next few days (Fig. 4E). At these very early stages of salt stress, Na⁺ content was only slightly increased in all plants, and Na⁺ content of the *Nt-cbl10a10b* double mutant accumulated at a similar rate as WT from 0 to 5 DAT (Fig. 4F). These results do not support a role for leaf Na⁺ accumulation and toxicity in the severe salt sensitivity phenotype of the *Nt-cbl10a10b*

double mutant. Ca²⁺ and Mg²⁺ contents were not significantly different between WT and mutants under both control and saline conditions (Supplementary Fig.S5C, S5D). In addition, the Na⁺/K⁺ ratios of WT and *Nt-cbl10a10b* double mutant under salt stress were also quite similar (Supplementary Fig.S5E), indicating the salt-sensitive phenotype of the double mutant is not likely because of an affected Na⁺/K⁺ ratio. Interestingly, Cl⁻ accumulated at a significantly lower rate in the *Nt-cbl10a10b* double mutant compared to WT (Fig. 4G), and the Na⁺/Cl⁻ accumulation ratio in the double mutant was much higher than that in the WT (Supplementary Fig.S5F).

4. The chlorosis of *NtCBL10* loss-of-function mutants under dark conditions

Previous reports have shown that some lesion-mimic phenotypes are connected to light or defective photosystems (Zulfugarov et al., 2014, Bruggeman et al., 2015, Wang et al., 2015, Tang et al., 2020). In the *Nt-cbl10a10b* double mutant, photosynthesis was affected already at a very early stage of salt treatment (Figs. 3C, 4D). We explored whether the salt-sensitive phenotype of the *Nt-cbl10a10b* double mutant leaves and the early-targeted degradation of chlorophyll was light-dependent in a dark treatment (whole plants were shaded from light simultaneously while undergoing salt treatment). Results showed that the *Nt-cbl10a10b* double mutant leaves suffered possibly even more from early chlorophyll breakdown and chlorosis of the leaf blades in the dark, but necrotic lesions were no longer visible (Figs. 5A, 5B). These results suggest that the salt stress-induced necrosis of the *Nt-cbl10a10b* double mutant leaves is dependent on light but the breakdown of chlorophyll is light-independent.

At the same time, Na⁺ accumulation rates of both WT and *Nt-cbl10a10b* double mutants were very low from 1 DAT to 6 DAT (Fig. 5D), which argues against a role for Na⁺ accumulation in the early chlorophyll breakdown of the salt-stressed *Nt-cbl10a10b* double mutant. Interestingly, the reduced rate of Cl⁻ accumulation in the *Nt-cbl10a10b* double mutant compared to WT observed under salt stress was reversed in the leaves grown in the dark (Figs. 4G, 5E). Similar to the plants grown under normal light conditions, Ca²⁺ and Mg²⁺ contents were not significantly different between WT and mutants under both control and

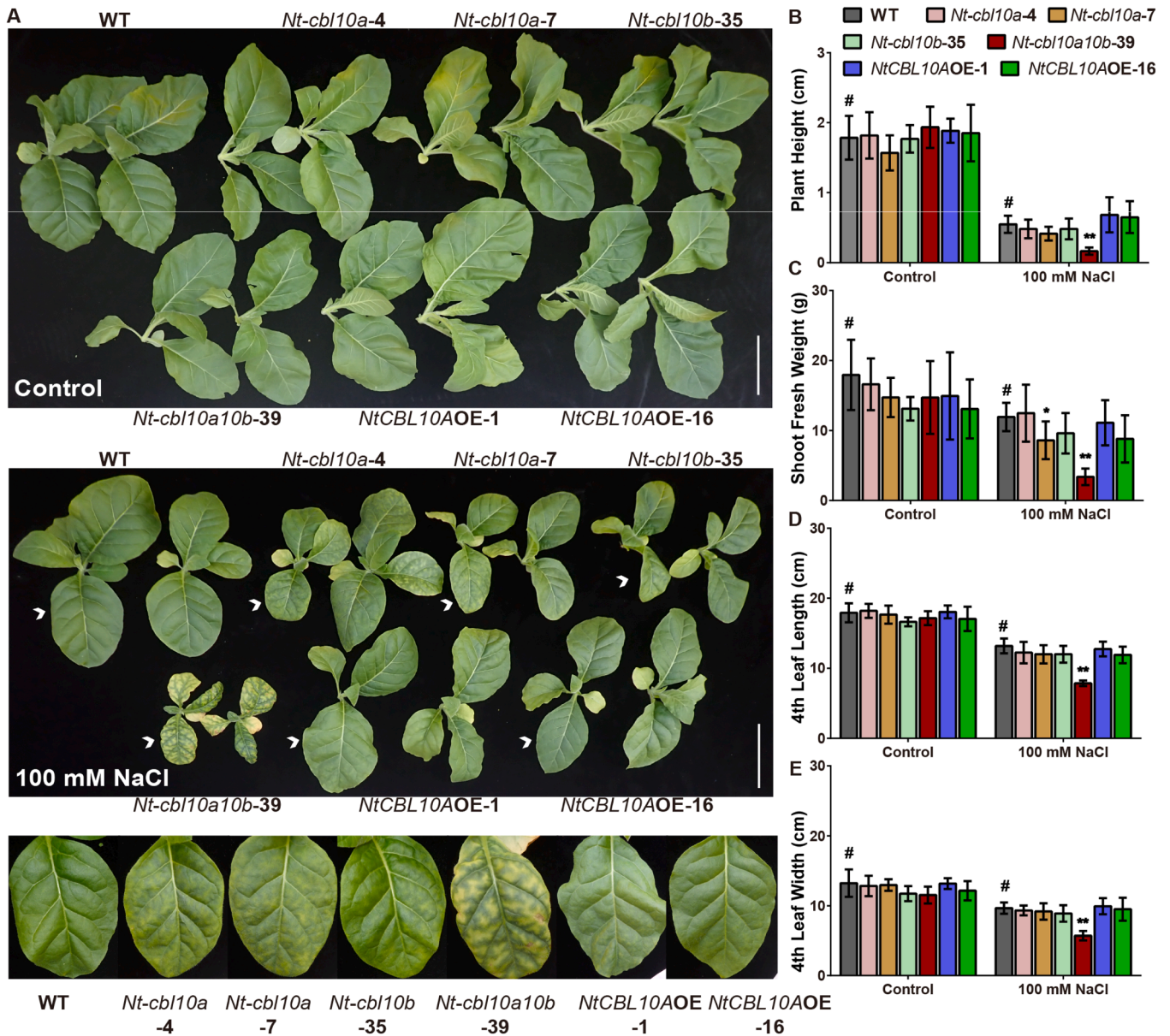


Fig. 2. The shoot phenotype of WT, *Nt-cbl10a* single mutant, *Nt-cbl10b* single mutant, *Nt-cbl10a10b* double mutant, and *NtCBL10AOE* lines under control conditions and salt stress (100 mM NaCl). Scale bars = 10 cm. (A) The shoot phenotype of plants at 8 DAT. White arrowheads indicate the 4th leaves which are zoomed in at the bottom part of the panel. (B-E) The plant height, shoot fresh weight, 4th leaf width, and 4th leaf length of all lines at 8 DAT (days after reaching 100 mM NaCl treatment). Error bars indicate \pm SD (n = 6). The # symbol indicates the WT value, and asterisks denote statistically significant differences between WT (#) and the transgenic plants under control or saline conditions, there will be no symbol for that value if there is no statistically significant difference between this group with WT (Student's *t*-test, **p* < 0.05 and ***p* < 0.01).

saline conditions in the dark (Supplementary Fig.S5C, S5D, S5G, S5H).

4. Discussion

The *CBL* gene family members are crucial participants in plant stress responses (Mao et al., 2022). In this study, knocking out *NtCBL10* in tobacco results in a severe salt-sensitive phenotype. The early breakdown of chlorophyll along with fast decreasing PhiPS2 suggests a direct devastating effect on photosynthetic components in the *Nt-cbl10a10b* double mutant. Interestingly, the severe salt-sensitive phenotype of the *Nt-cbl10a10b* double mutant includes very fast-developing chlorosis in addition to necrotic symptoms under light, while it only exhibited the chlorosis symptoms under salt stress under dark. These results indicate that the chlorosis phenotype is light-independent and the necrosis phenotype is light-dependent, and these combined phenotypes may be

caused by different disturbed pathways induced by the loss of *NtCBL10*. A possible explanation for this may be linked to the wide range of regulatory functions that *CBL10* appears to have in response to salt stress.

Notably, the diverse functions of CBL proteins closely tie to their subcellular localization, probably by recruiting different CIPKs to specific subcellular locations (Luan, 2009, Mao et al., 2023). AtCBL10 was found to be localized to the PM, endosomal, and tonoplast compartments (Kim et al., 2007, Quan et al., 2007, Batistic et al., 2010). Like AtCBL10, Both *NtCBL10A* and *NtCBL10B* were predicted to contain a transmembrane helix for membrane association (Mao et al., 2023). We do not have experimental evidence in this study of the subcellular location of *NtCBL10A* and *NtCBL10B*, but the possible subcellular locations of *NtCBL10* could be various. Based on the data in this study, we tried to understand the combined salt-sensitive phenotypes of *Nt-cbl10a10b* double mutants from the possible roles of CBL10 at various

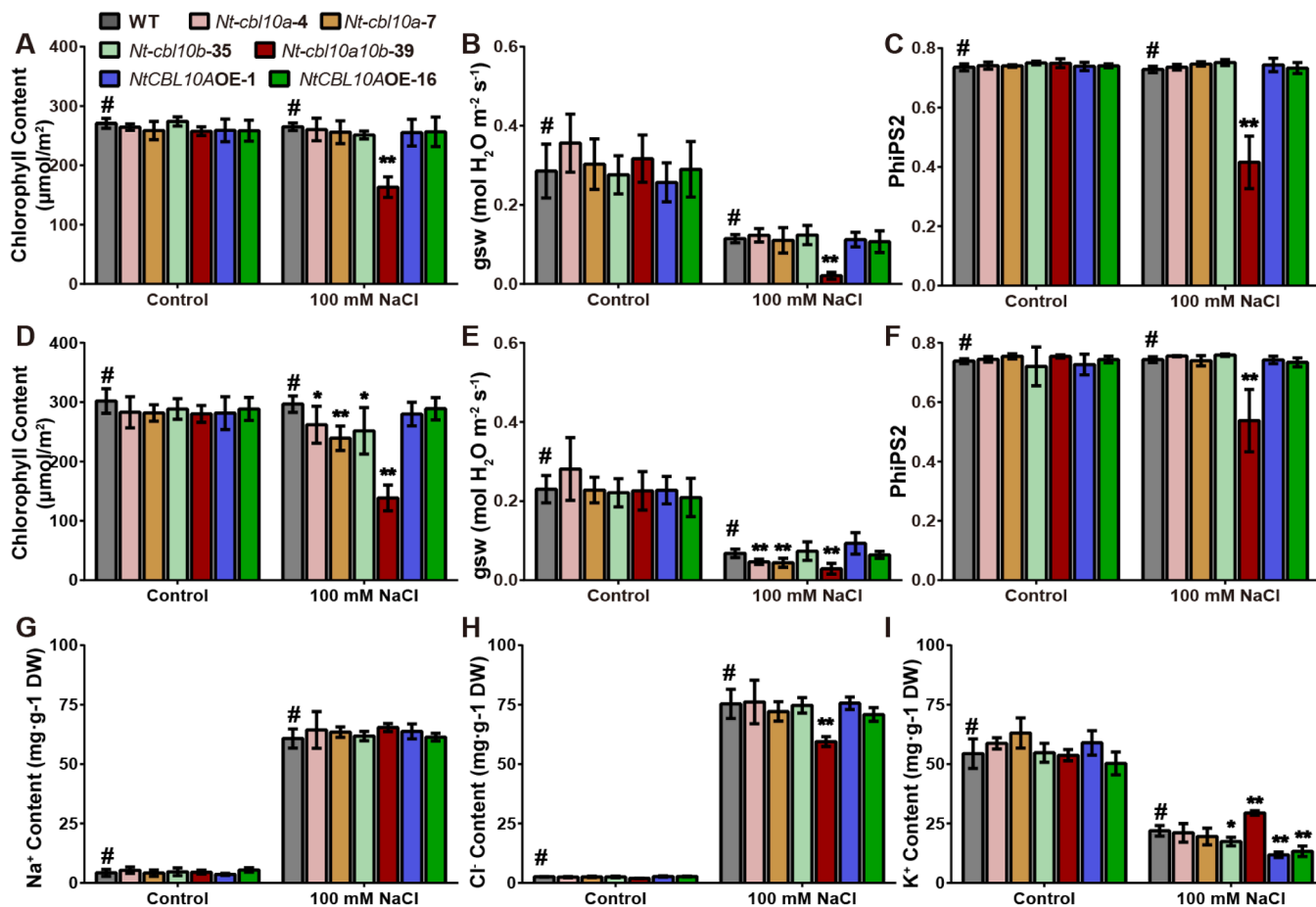


Fig. 3. The determination of physiological parameters of WT, *Nt-cbl10a*, *Nt-cbl10b* single mutants, *Nt-cbl10a10b* double mutant, and *NtCBL10AOE* lines under control conditions and salt stress (100 mM NaCl). (A-F) The chlorophyll content, stomatal conductance, and chlorophyll fluorescence of all lines at 3 DAT (days after reaching 100 mM NaCl treatment) (A-C) and 7 DAT (D-F). Error bars indicate \pm SD ($n = 6$). (G-I) Ion contents (Na^+ , Cl^- , and K^+) in leaf blades of all lines under control and saline conditions at 7 DAT. Error bars indicate \pm SD ($n = 4$). The # symbol indicates the WT value, and asterisks denote statistically significant differences between WT (#) and the transgenic plants under control or saline conditions, there will be no symbol for that value if there is no statistically significant difference between this group with WT (Student's *t*-test, * $p < 0.05$ and ** $p < 0.01$).

organelles.

4.1. The light-dependent necrotic phenotype of *Nt-cbl10a10b* double mutant

4.1.1. Na^+ homeostasis regulation at membrane and tonoplast

A role for CBL10 together with CIPK24 in regulating Na^+ transport over the tonoplast was proposed in *Arabidopsis* (Kim et al., 2007). It was suggested that the tonoplast-localized CBL10-CIPK24 complex regulates Na^+ sequestration into the vacuole (Kim et al., 2007, Plasencia et al., 2020). If this pathway is also established in tobacco, the *Nt-cbl10a10b* double mutants may accumulate excessive Na^+ in the cytosol because Na^+ is not efficiently transported to the vacuole, even though the initial increase in whole leaf Na^+ content of mutants was quite similar to that of WT plants (Fig. 4F). In addition, CBL10 also affects Na^+ transport over the PM as part of the SOS pathway (Plasencia et al., 2020). AtCBL10-AtCIPK8 and AtCBL10-AtCIPK24 modules appear to be able to interact with SOS1 activity of extruding Na^+ into the apoplast (Quan et al., 2007, Lin et al., 2009, Yin et al., 2019). The loss of Na^+ extruding activity of *Nt-cbl10a10b* double mutant together with reduced Na^+ sequestration in the vacuole may contribute to a much higher relative Na^+ concentration in the cytosol.

This hypothesis of disturbed Na^+ homeostasis resulting in Na^+ accumulation in the cytosol seems in line with the fact that the necrotic symptoms of *Nt-cbl10a10b* double mutant under salt stress are light-

dependent. Plants grown under dark conditions transpire much less than plants grown under light, which will influence the transpiration flow (Supplementary Fig. S6). This is likely to affect the accumulation rate of Na^+ in the leaves: Na^+ is transported to the leaf blades with the transpiration stream and is deposited there under continuous salt stress, and only a small proportion of the Na^+ is recirculated to roots through phloem for most plants (Tester and Davenport., 2003). Therefore, it is likely that Na^+ ions accumulate faster in plant leaves under light conditions (with high transpiration flow) than under dark conditions, which is evidenced by the leaf Na^+ measurements in light and dark-treated leaves (Figs. 4F, 5D). In this case, the appearance of necrotic symptoms of *Nt-cbl10a10b* double mutant may be delayed in the dark. However, at 6 DAT, the double mutant accumulated approximately $40 \text{ mg}\cdot\text{g}^{-1}$ DW Na^+ in the dark (Fig. 5D), which is comparable to the Na^+ levels observed at 2 DAT in the light (Fig. 4F), when necrotic spots had already formed (Fig. 4A). Additionally, during our observations until the plants died at 15 DAT (data not shown), no necrosis was detected in the dark. Therefore, in addition to transpiration-affected Na^+ accumulation, other light-associated factors may also be involved in necrosis formation.

4.1.2. Cl^- homeostasis regulation at the chloroplast

Cl^- is an essential micronutrient for tobacco but can accumulate to macronutrient levels, functioning as an essential macronutrient (Brumos et al., 2010). It has been reported that Cl^- plays specific roles in

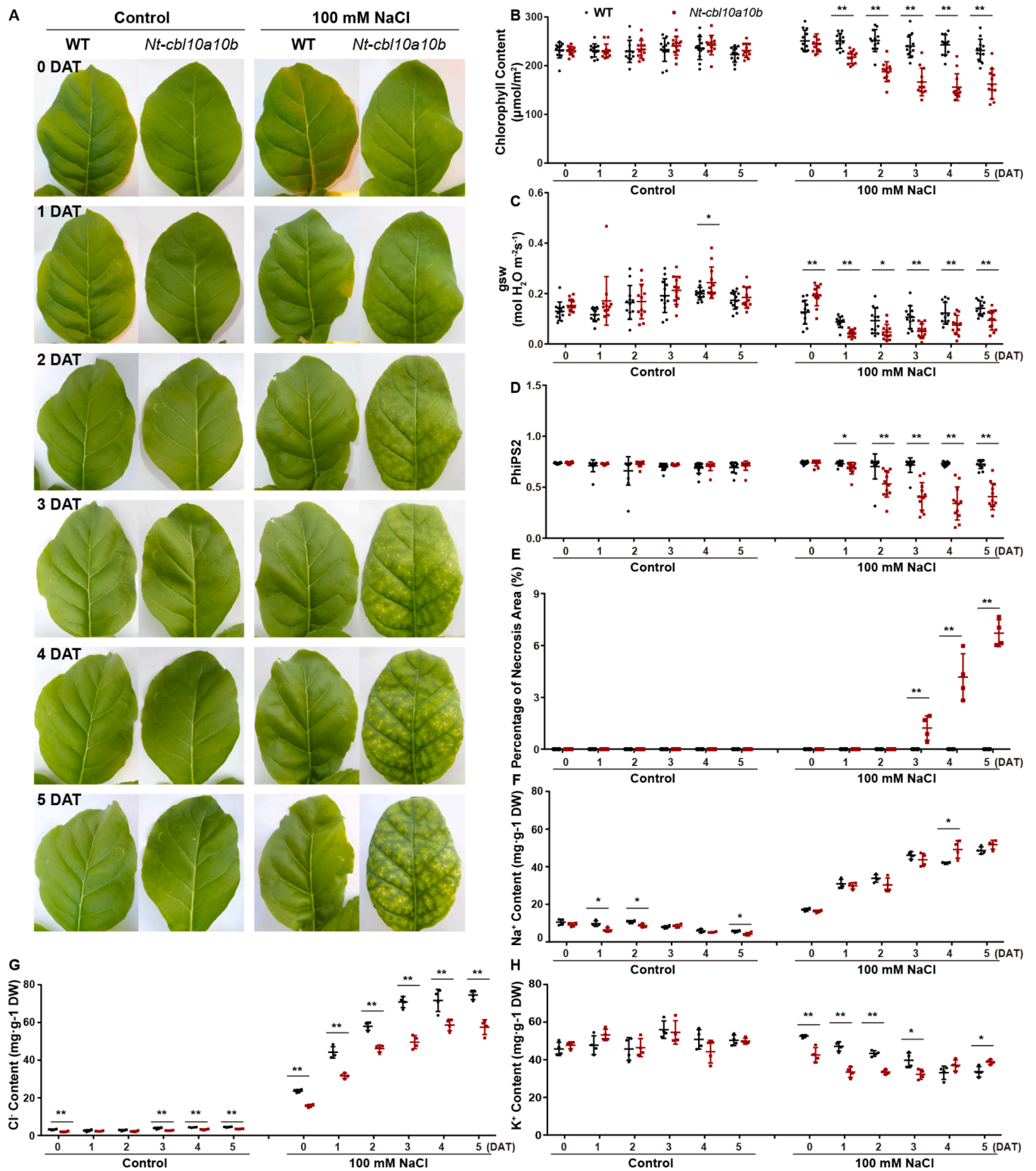


Fig. 4. The phenotype and physiological parameters of WT and *Nt-cbl10a10b* double mutant on different time points after salt treatment (100 mM NaCl). (A) The shoot phenotype of plants at 0–5 DAT (days after reaching 100 mM NaCl treatment). (B–D) The chlorophyll content, stomatal conductance, and chlorophyll fluorescence of all lines at 0–5 DAT. Error bars indicate \pm SD ($n = 12$). (E–H) Necrosis quantification and Ion contents (Na^+ , Cl^- , and K^+) in leaf blades of all lines under control and saline conditions at 0–5 DAT. Error bars indicate \pm SD ($n = 4$). Asterisks indicate statistically significant differences of *Nt-cbl10a10b* double mutant compared with WT under control or saline conditions at different time points (Student’s *t*-test, * $p < 0.05$ and ** $p < 0.01$).

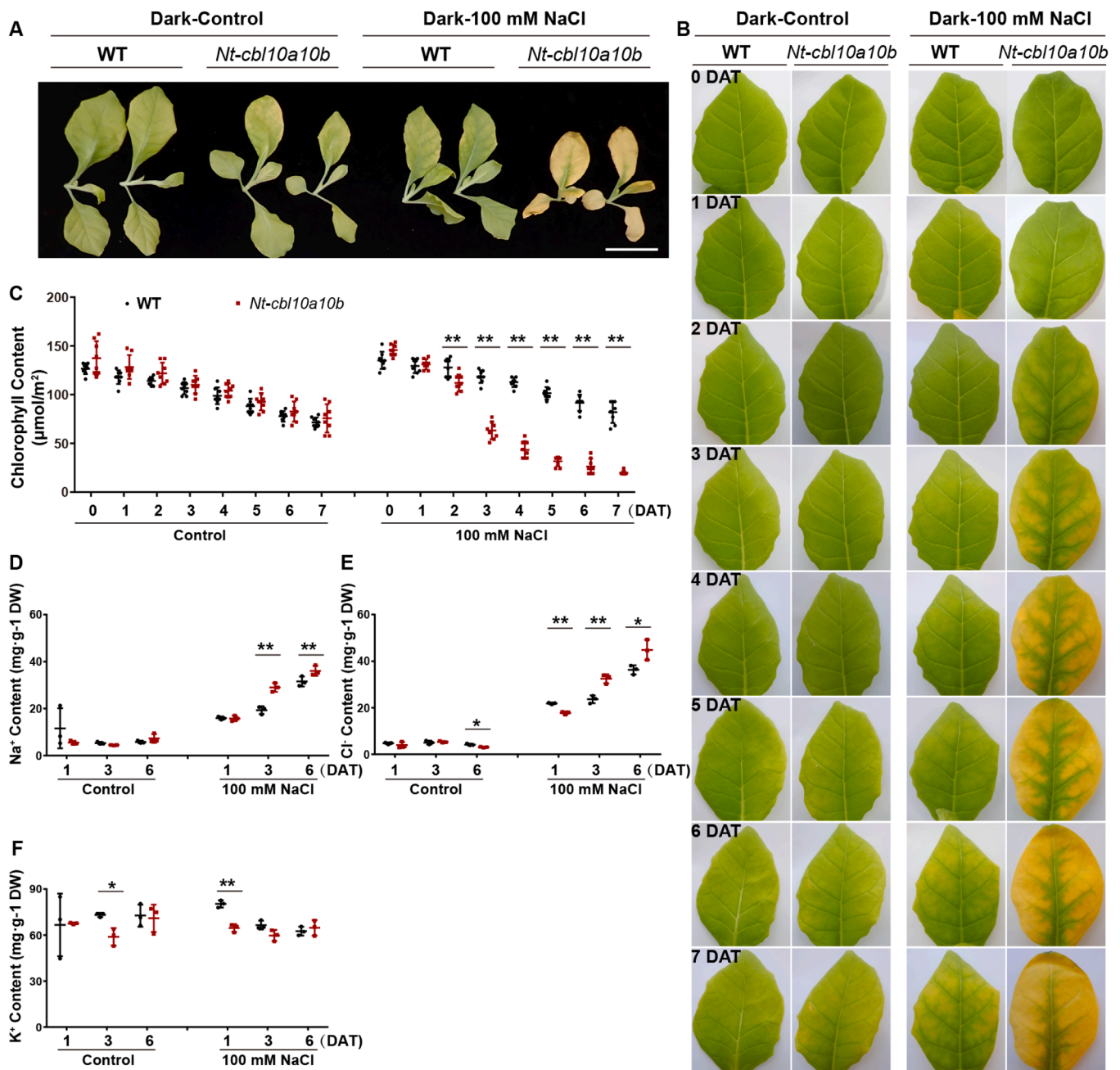


Fig. 5. The phenotype and physiological parameters of WT and *Nt-cbl10a10b* double mutant on different time points after salt treatment (100 mM NaCl) in the dark. (A) The shoot phenotype of plants at 7 DAT (days after reaching 100 mM NaCl treatment). (B) The shoot phenotype of plants at 0–7 DAT. (C) The chlorophyll content of all lines at 0–7 DAT. Error bars indicate \pm SD ($n = 8$). (D–F) Ion contents (Na^+ , Cl^- , and K^+) in leaf blades of all lines under control and saline conditions at 1, 3, and 6 DAT. Error bars indicate \pm SD ($n = 3$). Asterisks indicate statistically significant differences of *Nt-cbl10a10b* double mutant compared with WT under control or saline conditions at different time points (Student's *t*-test, * $p < 0.05$ and ** $p < 0.01$).

regulating leaf osmotic potential and turgor when accumulated to a macronutrient concentration of $51.08 \text{ mg}\cdot\text{g}^{-1} \text{ DW}$ (Franco-Navarro et al., 2016). In our study, the leaf Cl^- concentration of plants under salt stress was close to this value, suggesting that Cl^- may play a protective biological role in resisting salt stress. Additionally, the *Nt-cbl10a10b* double mutant accumulated significantly less Cl^- under salt stress compared to WT (Fig. 4G). This indicates that the protective function of Cl^- in tobacco under salt stress may be compromised in the *Nt-cbl10a10b* double mutant due to the loss of *NtCBL10*.

The significantly less accumulation of Cl^- in the *Nt-cbl10a10b* double mutant under salt stress does not seem to be caused by less xylem flow/transpiration even though the stomatal conductance of the *Nt-cbl10a10b*

double mutant is lower than that of WT (Figs. 3B and 3E), because the Na^+ accumulation between WT and mutant was not significantly different (Fig. 4F). Therefore, it may be related to Cl^- uptake in the roots or the efficiency of Cl^- root-to-shoot translocation. Whether CBL10 plays a role in Cl^- homeostasis is unknown, but a component of the CBL-CIPK network was reported to regulate the Cl^- root-to-shoot translocation. AtCBL1/9-AtCIPK23 can activate the anion channel SLOW-TYPE ANION CHANNEL (SLAC1) in *Xenopus oocytes*, which is a PM-localized channel that is highly permeable to malate and chloride in guard cells (Maierhofer et al., 2014). SLAC1 has four homologs, which are the SLAC1-associated homologs 1–4 (SLAH1 to SLAH4). SLAH3 can also be activated by AtCBL1/9-AtCIPK23 in *Xenopus oocytes*, and it can form

chloride-conducting heteromeric channels with SLAH1 in xylem-pole pericycle cells to regulate chloride root-to-shoot translocation (Maierhofer et al., 2014; Cubero-Font et al., 2016). AtCBL10 is reported to be able to interfere with AtCBL1/9-AtCIPK23 complexes by directly and competitively interacting with downstream targets. For instance, AtCBL10 competes with AtCBL1/9-AtCIPK23 in the interaction with AKT1 and represses the potassium uptake induced by AtCBL1/9-AtCIPK23 (Ren et al., 2013). Whether CBL1/9-CIPK23 also activates SLAC1 as well as its homologs (SLAH), and whether the reduced Cl⁻ accumulation in the leaves of the *Nt-cbl10a10b* double mutant under saline conditions is linked to the lack of CBL10 regulation of this mechanism is worth to explore.

Cl⁻ is the most abundant anion in the chloroplast stroma (50–90 mM) (Neuhaus and Wagner, 2000). The chloroplast envelopes and the thylakoid membrane exhibit a high permeability for Cl⁻, a non-assimilating highly mobile anion, that is preferred by plants to balance the electric charges of important cations to stabilize the electric potential of cell membranes and regulate pH gradients (Ulrich and Heldt, 1981; Bose et al., 2017; Colmenero-Flores et al., 2019). Cl⁻ influx from the stroma to the lumen is essential for thylakoid swelling after the onset of illumination, and Cl⁻ efflux to the stroma would cause the thylakoid to shrink during the transition to darkness (Colmenero-Flores et al., 2019). In addition, the accumulated protons in the thylakoid lumen can be electrically counterbalanced by Cl⁻ influx, thus possibly regulating the pH gradient between the lumen and the stroma. Cl⁻ homeostasis in the *Nt-cbl10a10b* double mutant may be disrupted due to the loss of *NtCBL10*, possibly affecting the ability of Cl⁻ to protect PSII (Colmenero-Flores et al., 2019; Cakmak et al., 2023). Interestingly, the reduced rate of leaf Cl⁻ accumulation in the *Nt-cbl10a10b* double mutant compared to WT under salt stress was reversed in the leaves grown in the dark (Figs. 4G, 5E), while the necrotic lesions disappeared. Whether there is any connection between Cl⁻ accumulation in *Nt-cbl10a10b* and the necrotic phenotype remains to be established, but would be interesting to explore.

4.1.3. Reactive oxygen species (ROS)

Under salt stress, the Calvin cycle is inhibited by salinity-induced stomatal closure, leading to the over-reduction of the electron transport chain and the generation of ROS (Attia et al., 2009; Hajiboland, 2014; Shi, 2023). Our results showed that the stomatal conductance of *Nt-cbl10a10b* double mutant was severely inhibited by salt stress since 1 DAT (Fig. 4C). Possibly, the light energy input in *Nt-cbl10a10b* leaves may exceed energy utilization when the Calvin cycle is more inhibited than the light reaction in the photosynthesis of *Nt-cbl10a10b* leaves under salt stress. Therefore, the resulting ROS generation in *Nt-cbl10a10b* leaves might exceed the ROS scavenging ability, leading to necrotic lesions. This hypothesis would be in line with the reduction of necrotic lesions in the dark, without photon capture, the imbalance between photon capture and energy utilization is absent, and therefore generation of ROS and the resulting necrotic lesions would be significantly reduced.

4.2. The light-independent chlorotic phenotype of *Nt-cbl10a10b* double mutant

In contrast to the necrosis, the chlorosis symptoms of the *Nt-cbl10a10b* double mutant were shown to be light-independent, or even exacerbated in the dark (Fig. 5B). Although we cannot rule out a role for cytosolic Na⁺ accumulation in the development of the chlorotic symptoms, the low rate of Na⁺ accumulation in the leaves of *Nt-cbl10a10b* double mutant grown in the dark while chlorotic symptoms still developed very fast suggests that Na⁺ accumulation itself may not be causal to the chlorosis and fast breakdown of chlorophyll. So then the question remains: what causes the extreme and fast-developing chlorosis in the *Nt-cbl10a10b* double mutant?

4.2.1. H⁺ homeostasis regulation at tonoplast and TGN/EE

Salt stress induces cytosolic pH fluctuations mediated by ion/H⁺ exchangers, cotransporters, and proton pumps (Kader et al., 2007; Pittann et al., 2009; Zhou et al., 2021). Subsequently, these changes may influence vacuolar pH dynamics due to proton movement between the cytosol and the vacuole (Kader et al., 2007). It is reported that salt-induced changes in cytosolic pH may affect photosynthetic activity in tobacco plants (Pecherina et al., 2022).

CBL10 also appears to be involved in the regulation of H⁺ homeostasis by amongst others affecting the activity of the vacuolar H⁺-ATPase (V-ATPase, VHA) and the vacuolar H⁺-pyrophosphatase (V-PPase, AVP1), which are two vital proton pumps in the tonoplast for energizing ion transport (Cosse and Seidel, 2021). VHA consists of two sub-complexes which are the peripheral V₁ complex (eight subunits VHA-A to -H) for ATP hydrolysis and the membrane-integral V₀ complex (VHA-a, -c, -c', -c'', -d, and -e) for proton translocation (Cipriano et al., 2008). AtCIPK24 was reported to interact with the peripheral VHA-B subunits and stimulate H⁺ transport activity (Batelli et al., 2007). In addition, in a tomato *Sl-cbl10* mutant, the gene expression of the vacuolar H⁺ pumps *SLAVP1* and *SLVHA-A1* was downregulated under saline conditions compared to WT (Egea et al., 2018), suggesting that *SICBL10* affects H⁺ homeostasis, possibly as a driver for Na⁺ compartmentation into the vacuole. Therefore, the CBL10-CIPK24 complex may contribute to Na⁺ compartmentation by stimulating the tonoplast-localized proton pumps (regulating the H⁺ homeostasis). Furthermore, AtCBL10 was also suggested to negatively regulate the activity of AtAHA4 and AtAHA11 in an AtCIPK-independent manner (by direct interaction) in *Arabidopsis* (Xie et al., 2022). Impaired regulation of the H⁺ pumps under saline conditions may result in impaired H⁺ homeostasis and pH regulation, which can be highly damaging to the leaf cell functioning, and even induce chlorophyll breakdown (Long et al., 2017).

Interestingly, a VHA-deficient *det3* mutant showed severe salt sensitivity (Batelli et al., 2007), but this salt sensitivity was evidenced later to be caused by reduced VHA activity in the trans-Golgi network/early endosome (TGN/EE) but not at the tonoplast. A loss-of-function mutant of *VHA-a2* and *VHA-a3* (two VHA-a isoforms localized in the tonoplast) did not show salt sensitivity and still accumulated Na⁺, while the loss-of-function of *VHA-a1* (an isoform localized in the TGN/EE) was salt-supersensitive (Krebs et al., 2010). The TGN/EE is an organelle with complex cellular roles, one of which is sorting and delivering proteins to the apoplast, PM, and vacuole. Plant cells always maintain a low luminal pH, and the impaired TGN/EE pH regulation may lead to severe plant growth defects (McKay et al., 2022).

These studies indicate that the vacuole and endosomal system contribute to regulating H⁺ homeostasis, and that this is particularly important for salt tolerance of plants. Whether impaired pH regulation is causal to the fast-developing chlorosis in the *Nt-cbl10a10b* double mutant under salt stress remains to be established.

4.2.2. CBL10 and chloroplast-localized proteins

CBL10 was also found to directly interact with and repress the TOC34 protein, a member of the TOC (translocon of the outer membrane of the chloroplasts) complex with GTPase activity to regulate protein import into chloroplasts (Cho et al., 2016). This study evidenced the subcellular localization of CBL10 at the chloroplast and indicated that CBL10 may play a role in chloroplast functions, which seems in line with our result that the knockout of *NtCBL10* leads to fast chlorophyll breakdown and PSII defects under salt stress. The importance of maintaining ion homeostasis in the different cellular organelles under salt stress conditions cannot be overstated, and the putative role of CBL-CIPK network components in the correct functioning of chloroplasts as well as TGN/EE organelles under stress conditions is certainly worth exploring.

Another possible link between the CBL-CIPK network and chlorophyll was reported in a recent study, in which AtCIPK24 was shown to interact with phytochrome-interacting factors PIF1 and PIF3 in the nucleus, phosphorylating them and decreasing their stability (Ma et al.,

2023). PIFs are bHLH-family transcription factors that act as negative regulators of photomorphogenesis (Pham et al., 2018). It has been shown that *PIF1* negatively regulates the expression of genes encoding protochlorophyllide oxidoreductase, ferrochelatase, and heme oxygenase in the chlorophyll biosynthetic pathway in the dark (Moon et al., 2008). Additionally, *PIF3* negatively regulates the expression of genes encoding key regulatory enzymes in the chlorophyll biosynthetic pathway and genes encoding PSI components (Shina et al., 2009). If the phosphorylation of PIF1 and PIF3 by CIPK24 depends on CBL10, the knockout of *CBL10* may alleviate the repressive effect of CIPK24 on PIF1 and PIF3, thus negatively regulating the chlorophyll biosynthetic pathway.

4.3. The role of *CBL10* and K^+ homeostasis

CBL10 also functions as a repressor by directly interacting with targets in a CIPK-independent way. AtCBL10 was reported to competitively interact with AKT1 against the AtCBL1/9-AtCIPK23 complex, repressing the potassium uptake regulated by AtCBL1/9-AtCIPK23 (Ren et al., 2013). This mechanism explained the observation that AtCBL10OE lines showed a low- K^+ sensitive phenotype and had reduced K^+ content under low- K^+ conditions (Ren et al., 2013). Our results showed that constitutive overexpression of *NtCBL10A* in *NtCBL10AOE* lines resulted in higher K^+ accumulation compared with WT under salt stress (Fig. 3I). This result may be in line with the previous report of competition between CBL10 and AKT1. However, we should emphasize that *NtCBL10A* is overexpressed under a constitutive promoter that drives expression in all tissues, developmental stages, and conditions. The overexpression of a gene, in particular a gene whose expression is normally limited to specific conditions or specific cell types, can cause inhibition or activation of a protein complex or pathway that it normally would not interact with (Prelich, 2012). Evidence supporting the role of *NtCBL10* in K^+ accumulation comes from studies of the *Nt-cbl10a10b* double mutants. The observed difference in K^+ accumulation between the WT and the double mutant suggests that *NtCBL10* influences K^+ accumulation under salt stress conditions (Figs. 3I, 4H). However, this effect changes over the course of salt treatment. In the early phase (0–3 DAT), K^+ accumulation in the double mutant is significantly lower than in the WT, but the difference diminishes over time (Fig. 4H). Intriguingly, by 5 and 7 DAT, K^+ accumulation in the double mutant exceeds that of the WT (Figs. 3I, 4H). The Na^+/K^+ ratios in WT and *Nt-cbl10a10b* are always similar during 0–5 DAT (Supplementary Fig.S5E). These results indicate that K^+ homeostasis is affected by the loss of *NtCBL10*, but its variation over time during salt stress is complex and may be a consequence rather than a cause of salt sensitivity.

5. Concluding remarks

The results presented in this paper show that *NtCBL10* plays a pivotal role in the salt stress response of tobacco. The extremely fast-developing chlorosis and necrosis symptoms in leaves of the *NtCBL10* functional knockout plants point to a regulatory role for *CBL10*, possibly in concert with several CIPK partners, for the adaptation of ion homeostasis under saline conditions. This may include not only regulation of organellar and cellular membrane transport of Na^+ and Cl^- ions, but also maintaining proton gradients over organellar membranes that are essential for the proper functioning of the cells and protection of photosynthetic processes.

Funding information

This work was supported by the National Natural Science Foundation of China (32170387); the Agricultural Science and Technology Innovation Program (ASTIP-TRIC02); Funding of WNTC (2023341800040464) and XZ-CTID; the Collaborative Science and Technology Project of JSZY (H202422).

Authors contribution

J.M. designed the research plan, carried out the experiments, and analyzed the data; J.M., C.G.V.L., and Q.W. completed the writing; Y.N., Q.W., and C.G.V.L. co-supervised the writing; G.Y., G.X., L.X., and D.M. and H.L. provided ideas and joined discussion; R.G.F.V. and Y.B. helped with manuscript revision. Y.N. and Q.W. agree to serve as the authors responsible for contact and ensure communication. All authors contributed to the article and approved the submitted version.

CRediT authorship contribution statement

Qian Wang: Writing – review & editing, Supervision, Funding acquisition. **C. Gerard van der Linden:** Writing – review & editing, Supervision, Methodology, Formal analysis. **Jingjing Mao:** Writing – original draft, Formal analysis, Data curation, Conceptualization. **Guang Yuan:** Formal analysis. **Richard G.F. Visser:** Writing – review & editing, Supervision. **Yuling Bai:** Writing – review & editing, Supervision. **Gang Xu:** Resources. **Lin Xue:** Resources. **Dongping Mao:** Resources. **Haobao Liu:** Writing – review & editing, Supervision. **Yang Ning:** Supervision, Resources, Funding acquisition.

Declaration of Competing Interest

The authors declare that they have no known competing financial interests or personal relationships that could have appeared to influence the work reported in this paper.

Acknowledgments

We would like to acknowledge the support of the PhD Education Programs between The GSCAAS and WUR.

Appendix A. Supporting information

Supplementary data associated with this article can be found in the online version at doi:10.1016/j.envexpbot.2024.106083.

References

- Attia, H., Karray, N., Lachaal, M., 2009. Light interacts with salt stress in regulating superoxide dismutase gene expression in Arabidopsis. *Plant Sci.* 177 (3), 161–167.
- Batelli, G., Verslues, P.E., Agius, F., et al., 2007. SOS2 promotes salt tolerance in part by interacting with the vacuolar H^+ -ATPase and upregulating its transport activity. *Mol. Cell. Biol.* 27 (22), 7781–7790.
- Batistic, O., Waadt, R., Steinhilber, L., et al., 2010. CBL-mediated targeting of CIPKs facilitates the decoding of calcium signals emanating from distinct cellular stores. *Plant J.* 61 (2), 211–222.
- Bose, J., Munns, R., Shabala, S., et al., 2017. Chloroplast function and ion regulation in plants growing on saline soils: lessons from halophytes. *J. Exp. Bot.* 68 (12), 3129–3143.
- Bruggeman, Q., Raynaud, C., Benhamed, M., et al., 2015. To die or not to die? Lessons from lesion mimic mutants. *Front. Plant Sci.* 6, 24.
- Brumos, J., Talon, M., Bouhlal, R., et al., 2010. Cl^- homeostasis in inclusion and excluder citrus rootstocks: transport mechanisms and identification of candidate genes. *Plant, Cell Environ.* 33 (12), 2012–2027.
- Cakmak, I., Brown, P., Colmenero-Flores, J.M., et al., 2023. Micronutrients. Marschner's mineral nutrition of plants. Academic Press, pp. 283–385.
- Cho, J.H., Lee, J.H., Park, Y.K., et al., 2016. Calcineurin B-like protein CBL10 directly interacts with TOC34 (translocator of the outer membrane of the chloroplasts) and decreases its GTPase activity in Arabidopsis. *Front. Plant Sci.* 7, 1911.
- Cipriano, D.J., Wang, Y., Bond, S., et al., 2008. Structure and regulation of the vacuolar ATPases. *Biochim. Et. Biophys. Acta* 1777 (7–8), 599–604.
- Colmenero-Flores, J.M., Franco-Navarro, J.D., Cubero-Font, P., et al., 2019. Chloride as a beneficial macronutrient in higher plants: new roles and regulation. *Int. J. Mol. Sci.* 20 (19), 4686.
- Cosse, M., Seidel, T., 2021. Plant proton pumps and cytosolic pH-homeostasis. *Front. Plant Sci.* 12, 672873.
- Cubero-Font, P., Maierhofer, T., Jaslan, J., et al., 2016. Silent s-type anion channel subunit slah3 gates slah3 open for chloride root-to-shoot translocation. *Curr. Biol.* 26 (16), 2213–2220.
- Egea, I., Pineda, B., Ortiz-Atienza, A., et al., 2018. The SICBL10 calcineurin B-like protein ensures plant growth under salt stress by regulating Na^+ and Ca^{2+} homeostasis. *Plant Physiol.* 176 (2), 1676–1693.

- Franco-Navarro, J.D., Brumos, J., Rosales, M.A., et al., 2016. Chloride regulates leaf cell size and water relations in tobacco plants. *J. Exp. Bot.* 67 (3), 873–891.
- Góral, T., 2023. Application of the detached-leaf technique to evaluate the pathogenicity of isolates of fungi *Ascochyta fabae* and *Botrytis fabae* to faba bean. *Biul. Inst. Hod. i Aklim. Rošlin.* 299, 55–64.
- Hajiboland, R., 2014. Reactive oxygen species and photosynthesis. Oxidative damage to plants. P. Ahmad, the United States of America. Elsevier, pp. 1–63.
- Horsch, R.B., Fry, J.E., Hoffmann, N.L., et al., 1985. A simple and general method for transferring genes into plants. *Science* 227, 1229–1231.
- Kader, M.A., Lindberg, S., Seidel, T., et al., 2007. Sodium sensing induces different changes in free cytosolic calcium concentration and pH in salt-tolerant and -sensitive rice (*Oryza sativa*) cultivars. *Physiol. Plant.* 130 (1), 99–111.
- Kim, B.-G., Waadt, R., Cheong, Y.H., et al., 2007. The calcium sensor CBL10 mediates salt tolerance by regulating ion homeostasis in *Arabidopsis*. *Plant J.* 52 (3), 473–484.
- Krebs, M., Beyhl, D., Gorlich, E., et al., 2010. Arabidopsis V-ATPase activity at the tonoplast is required for efficient nutrient storage but not for sodium accumulation. *Proc. Natl. Acad. Sci. USA* 107 (7), 3251–3256.
- Li, B., Shang, Y., Wang, L., et al., 2022. Highly efficient multiplex genome editing in dicots using improved CRISPR/Cas systems. *bioRxiv*, 2022–01.
- Lin, H.X., Yang, Y.Q., Quan, R.D., et al., 2009. Phosphorylation of SOS3-LIKE CALCIUM BINDING PROTEIN8 by SOS2 protein kinase stabilizes their protein complex and regulates salt tolerance in *Arabidopsis*. *Plant Cell* 21 (5), 1607–1619.
- Liu, Q., Wang, C., Jiao, X., et al., 2019. Hi-TOM: a platform for high-throughput tracking of mutations induced by CRISPR/Cas systems. *Sci. China Life Sci.* 62, 1–7.
- Livak, K.J., Schmittgen, T.D., 2001. Analysis of relative gene expression data using real-time quantitative PCR and the $2^{-\Delta\Delta Ct}$ method. *Methods* 25 (4), 402–408.
- Long, A., Zhang, J., Yang, L.T., et al., 2017. Effects of low pH on photosynthesis, related physiological parameters, and nutrient profiles of citrus. *Front Plant Sci.* 8, 185.
- Luan, S., 2009. The CBL-CIPK network in plant calcium signaling. *Trends Plant Sci.* 14 (1), 37–42.
- Ma, L., Han, R., Yang, Y., et al., 2023. Phytochromes enhance SOS2-mediated PIF1 and PIF3 phosphorylation and degradation to promote Arabidopsis salt tolerance. *Plant Cell* 35 (8), 2997–3020.
- Maierhofer, T., Diekmann, M., Offenborn, J.N., et al., 2014. Site- and kinase-specific phosphorylation-mediated activation of SLAC1, a guard cell anion channel stimulated by abscisic acid. *Sci. Signal.* 7 (342) ra86–ra86.
- Mao, J., Mo, Z., Yuan, G., et al., 2022. The CBL-CIPK network is involved in the physiological crosstalk between plant growth and stress adaptation. *Plant Cell Environ.* 46 (10), 3012–3022.
- Mao, J., Yuan, G., Han, K., et al., 2023. Genome-wide identification of CBL family genes in *Nicotiana tabacum* and the functional analysis of *NtCBL4A-J* under salt stress. *Environ. Exp. Bot.* 209, 105311.
- Mao, J., Yuan, J., Mo, Z., et al., 2021. Overexpression of *NtCBL5A* leads to necrotic lesions by enhancing Na^+ sensitivity of tobacco leaves under salt stress. *Front. Plant Sci.* 12, 740976.
- Masaló, I., Oca, J., 2020. Evaluation of a portable chlorophyll optical meter to estimate chlorophyll concentration in the green seaweed *Ulva ohnoi*. *J. Appl. Phycol.* 32 (6), 4171–4174.
- McKay, D.W., McFarlane, H.E., Qu, Y., et al., 2022. Plant trans-golgi network/early endosome pH regulation requires Cation Chloride Cotransporter (CCC1). *Elife* 11, e70701.
- Monihan, S.M., Ryu, C.H., Magness, C.A., et al., 2019. Linking duplication of a calcium sensor to salt tolerance in *Eutrema salsugineum*. *Plant Physiol.* 179 (3), 1176–1192.
- Moon, J., Zhu, L., Shen, H., et al., 2008. PIF1 directly and indirectly regulates chlorophyll biosynthesis to optimize the greening process in *Arabidopsis*. *Proc. Natl. Acad. Sci.* 105 (27), 9433–9438.
- Neuhaus, H.E., Wagner, R., 2000. Solute pores, ion channels, and metabolite transporters in the outer and inner envelope membranes of higher plant plastids. *Biochim. Et Biophys. Acta* 1465 (1–2), 307–323.
- Nunez-Ramirez, R., Sanchez-Barrena, M.J., Villalta, I., et al., 2012. Structural insights on the plant salt-overly-sensitive 1 (SOS1) Na^+/H^+ antiporter. *J. Mol. Biol.* 424 (5), 283–294.
- Pecherina, A., Grinberg, M., Ageyeva, M., et al., 2022. Salt-induced changes in cytosolic pH and photosynthesis in tobacco and potato leaves. *Int. J. Mol. Sci.* 24 (1), 491.
- Pham, V.N., Kathare, P.K., Huq, E., 2018. Phytochromes and phytochrome interacting factors. *Plant Physiol.* 176 (2), 1025–1038.
- Pitann, B., Schubert, S., Mühling, K.H., 2009. Decline in leaf growth under salt stress is due to an inhibition of H^+ -pumping activity and increase in apoplastic pH of maize leaves. *J. Plant Nutr. Soil Sci.* 172 (4), 535–543.
- Plasencia, F.A., Estrada, Y., Flores, F.B., et al., 2020. The Ca^{2+} sensor calcineurin B-Like protein 10 in plants: emerging new crucial roles for plant abiotic stress tolerance. *Front Plant Sci.* 11, 599944.
- Prelich, G., 2012. Gene overexpression: uses, mechanisms, and interpretation. *Genetics* 190 (3), 841–854.
- Price E. (2021). Measuring stomatal conductance and chlorophyll fluorescence with the new LI-600 porometer/fluorometer. 2021 ASHS Annual Conference, ASHS.
- Qiu, Q.-S., Guo, Y., Dietrich, M.A., et al., 2002. Regulation of SOS1, a plasma membrane Na^+/H^+ exchanger in *Arabidopsis thaliana*, by SOS2 and SOS3. *Proc. Natl. Acad. Sci. USA* 99 (12), 8436–8441.
- Quan, R., Lin, H., Mendoza, I., et al., 2007. SCABP8/CBL10, a putative calcium sensor, interacts with the protein kinase SOS2 to protect *Arabidopsis* shoots from salt stress. *Plant Cell* 19 (4), 1415–1431.
- Ren, X.L., Qi, G.N., Feng, H.Q., et al., 2013. Calcineurin B-like protein CBL10 directly interacts with AKT1 and modulates K^+ homeostasis in *Arabidopsis*. *Plant J.* 74 (2), 258–266.
- Schmidt, G.W., Delaney, S.K., 2010. Stable internal reference genes for normalization of real-time RT-PCR in tobacco (*Nicotiana tabacum*) during development and abiotic stress. *Mol. Genet Genom.* 283 (3), 233–241.
- Shi, D., 2023. Morning twilight of crop breeding for sodic land. *The Innovation Life* 1 (2), 100020–1.
- Shi, H., Quintero, F.J., Pardo, J.M., et al., 2002. The putative plasma membrane Na^+/H^+ antiporter SOS1 controls long-distance Na^+ transport in plants. *Plant Cell* 14 (2), 465–477.
- Shina, J., Kima, K., Kangb, H., et al., 2009. Phytochromes promote seedling light responses by inhibiting four negatively-acting phytochrome-interacting factors. *Proc. Natl. Acad. Sci.* 106 (18), 7660–7665.
- Sun, H., Sun, X., Wang, H., et al., 2020. Advances in salt tolerance molecular mechanism in tobacco plants. *Hereditas* 157 (1), 1–6.
- Tang, Y., Gao, C.C., Gao, Y., et al., 2020. OsNSUN2-mediated 5-methylcytosine mRNA modification enhances rice adaptation to high temperature. *Dev. Cell* 53 (3), 272–286.
- Tester, M., Davenport, R., 2003. Na^+ tolerance and Na^+ transport in higher plants. *Ann. Bot.* 91 (5), 503–527.
- Ulrich, H., Heldt, H.W., 1981. The chloroplast envelope: structure, function, and role in leaf metabolism. *Annu. Rev. Plant Physiol.* 32 (1), 139–168.
- Wang, J., Ye, B.Q., Yin, J.J., et al., 2015. Characterization and fine mapping of a light-dependent leaf lesion mimic mutant 1 in rice. *Plant Physiol. Biochem* 97, 44–51.
- Xie, Q., Yang, Y., Wang, Y., et al., 2022. The calcium sensor CBL10 negatively regulates plasma membrane H^+ -ATPase activity and alkaline stress response in *Arabidopsis*. *Environ. Exp. Bot.* 194, 104752.
- Yin, X., Xia, Y., Xie, Q., et al., 2019. The protein kinase complex CBL10-CIPK8-SOS1 functions in *Arabidopsis* to regulate salt tolerance. *J. Exp. Bot.* 1801–1814.
- Zhou, J.-Y., Hao, D.-L., Yang, G.-Z., 2021. Regulation of cytosolic pH: the contributions of plant plasma membrane H^+ -ATPases and multiple transporters. *Int. J. Mol. Sci.* 22 (23), 12998.
- Zhou, Y., Xu, C., 2023. Miniature genome editors derived from engineering Cas9 ancestor. *The Innovation Life* 1 (1), 100008–1.
- Zulfugarov, I.S., Tovuu, A., Eu, Y.-J., et al., 2014. Production of superoxide from photosystem II in a rice (*Oryza sativa* L.) mutant lacking PsbS. *BMC Plant Biol.* 14, 1–15.